

A unified model in the pulsed laser ablation process

HU De-zhi*

Department of Basic Science, North China Institute of Science and Technology, Beijing 101601, China

(Received 3 January 2008)

In this unified model, we introduce the electron-phonon coupling time (t_{ie}) and laser pulse width (t_p). For long pulses, it can substitute for the traditional thermal conduction model; while for ultrashort pulses, it can substitute for the standard two-temperature model. As an example of the gold target, we get the dependence of the electron and ion temperature evolution on the time and position by solving the thermal conduction equation using the finite-difference time-domain (FDTD) method. It is in good agreement with experimental data. We obtain the critical temperature of the onset of ablation using the Saha equation and then obtain the theoretical value of the laser ablation threshold when the laser pulse width ranges from nanosecond to femtosecond timescale, which consists well with the experimental data.

CLC numbers: TN249 **Document code:** A **Article ID:** 1673-1905(2008)04-0311-6

DOI 10.1007/s11801-008-7145-0

With the development and the application of the ultra-short high-power laser, the effect of non-Fourier thermal conduction in pulsed laser ablation is noted as remarkable^[1]. Then the two-temperature models have been established to describe the new phenomenon^[2-4]. But for the long-pulse laser, we still adopt the traditional thermal conduction model (TCM)^[5-8]. As a result, it is a complicated question that there is no model suitable for the pulse width from nanosecond to femtosecond timescale.

In this paper, we present a unified model that can describe the thermal conduction phenomenon as the laser pulse width ranges from nanosecond to femtosecond timescale.

As an example of the gold target, we get the dependence of the electron and ion temperature evolution on the time and position by solving the thermal conduction equation using FDTD method. It is in good agreement with the experimental data.

Many experimental and theoretical studies demonstrate the presence of two different ablation mechanisms^[9]: thermal ablation and non-equilibrium ablation. If the laser pulse duration (t_p) is more than the electron-phonon coupling time, a material can go through the thermal melting and subsequent thermal phenomenon, so called thermal ablation. If the pulse width is smaller than this time (t_{ie}), the ablation mechanism is called non-equilibrium ablation. Usually, the electron-phonon coupling time (t_{ie}) is several picoseconds^[10,11].

When the laser irradiates the surface of the target, the electron absorbs considerable laser energy firstly because the electron mass is far smaller than the ion mass. The electron

energy increases sharply. At the same time, electrons exchange energy with each other by colliding. Then the electron subsystem reaches the thermal equilibrium after tens of femtoseconds. If the laser irradiates the target, the electron subsystem continues to absorb the laser energy. And its temperature increases continually. At the same time, the ion absorbs little energy. The ion temperature is almost unchanged. It induces the tremendous difference of the temperature between the ion and the electron subsystem. Therefore, there are eigen temperature of the electron subsystems (T_e) and that of ion subsystem (T_i) in the target. This is the physical background of building TTM. The corresponding laser ablation process is called non-equilibrium ablation (NEA), whose characters are the non-Fourier thermal conduction phenomenon.

The electron-ion interaction is usually called the electron-phonon (e-ph) coupling effect. Studies indicate that the electron transfers the energy to the ion by this approach gradually. So the temperature difference between the ion subsystem and the electron subsystem decreases gradually. After several picoseconds, two subsystem temperatures reach equilibrium. The relaxation time is called the e-ph coupling time t_{ie} . But the different materials have different e-ph coupling times. For the nanosecond laser, its pulse width is more than the e-ph coupling time t_{ie} . This kind of ablation is called thermal equilibrium ablation (TEA). Its characters satisfy the Fourier law. For the picosecond laser ablation process, the corresponding microscopic mechanism is very complex. Approximately, both of the two ablation mechanisms coexist.

Thus, it can be seen that the ratio of the e-ph coupling

* E-mail: wjswjshh@163.com

time t_{ie} and laser pulse width t_p is the key, which distinguishes the two kinds of mechanisms. As $t_{ie}/t_p \gg 1$, it is the non-equilibrium ablation. As $t_{ie}/t_p \ll 1$, it is the thermal equilibrium ablation. As $t_{ie}/t_p \sim 1$, it is the mix ablation.

Considering the above physical background, we present the unified equations, which can describe the thermal conduction phenomenon of high energy-laser ablation process with the laser pulse width ranging from nanosecond to femtosecond.

$$C_e \frac{\partial}{\partial t} T_e = \exp[-at_{ie}/t_p] \frac{\partial}{\partial x} k_e \frac{\partial}{\partial x} T_e - g(T_e - T_i) + A(x, t) , \quad (1)$$

$$C_i \frac{\partial}{\partial t} T_i = g(T_e - T_i) , \quad (2)$$

$$A(x, t) = (1 - R)q_0 q(t)b \exp[-bx] , \quad (3)$$

$$q(t) = \exp[-4 \ln(2)(t/t_p - 1)^2] , \quad (4)$$

where T_i and T_e are the electron and the ion temperature, respectively. C_i and C_e are the heat capacities (per unit volume) of the ion and electron subsystems. k_e is the thermal conductivities for the electron. $A(x, t)$ is the energy source due to the laser energy dissipation into the matter. g is the e-ph coupling coefficient. R is the surface reflectivity. b is the material absorption coefficient. q_0 is the maximum pulse power. $q(t)$ is the Gaussian temporal function of the laser beam intensity distribution^[12-14]. a is the required value related to the optical property of the material. This paper ascertains the value by comparing the theoretical result with the experimental data.

If $t_{ie} \gg t_p$, i.e. $\exp[-\alpha t_{ie}/t_p] \sim 0$, equations (1)-(2) can transfer into,

$$C_e \frac{\partial T_e}{\partial t} = A(x, t) - g(T_e - T_i) , \quad (5)$$

$$C_i \frac{\partial T_i}{\partial t} = g(T_e - T_i) . \quad (6)$$

It is in perfect accordance with TTM^[15].

If $t_{ie} \ll t_p$, i.e. $\exp[-\alpha t_{ie}/t_p] \sim 1$, the ablation is the thermal equilibrium ablation. The system keeps at the thermal equilibrium state. By using of $T_e = T_i$ and $C_v = C_e + C_i$, equations (1)-(2) can be abbreviated as

$$C_v \frac{\partial T}{\partial t} = \frac{\partial}{\partial x} k \frac{\partial T}{\partial x} + A(x, t) . \quad (7)$$

It is in accordance with TCM.

If $t_{ie}/t_p \sim 1$, it is the mix ablation. The unified model can describe the whole conduction phenomenon better than other

models, i.e. TTM and the traditional thermal conduction model. Hence, the unified model can well describe the whole thermal conduction phenomenon with the laser pulse width ranging from nanosecond to femtosecond timescale.

According to the principle of energy conservation, the boundary condition on the target surface is as follows,

$$-k_s \frac{\partial T_s(x, t)}{\partial x} \Big|_{x=0} = bq(t) \quad (0 < t \leq t_p) . \quad (8)$$

Then according to the adiabatic condition, the boundary can be depicted as

$$\frac{\partial T_s(x, t)}{\partial x} \Big|_{x=\delta} = 0 \quad (0 < t \leq t_p) , \quad (9)$$

where δ is the maximum thermal conduction depth in a single pulse duration.

The initial temperature of the target is

$$T_s \Big|_{t=0} = T_0 . \quad (10)$$

So far, we present the unified model with the corresponding boundary conditions (8)-(9) and initial condition (10).

According to the above boundary conditions and initial condition, we discretize equations (1)-(4) using the finite-difference time-domain (FDTD) method.

At (i, j) , the corresponding equations are

$$\exp(-at_{ie}/t_p) k_e \frac{T_e(i+1, j+1) + T_e(i-1, j+1) - T_e(i, j+1)}{(\Delta x)^2} - g[T_e(i, j+1) - T_i(i, j+1)] + A(i\Delta x, j\Delta t) = C_e \frac{T_e(i, j+1) - T_e(i, j)}{\Delta t} , \quad (11)$$

$$C_i \frac{T_i(i, j+1) - T_i(i, j)}{\Delta t} = g[T_e(i, j+1) - T_i(i, j+1)] ,$$

$$A(i\Delta x, j\Delta t) = (1 - R)\alpha q(j\Delta t) \exp[-\alpha i\Delta x] ,$$

$$q(j\Delta t) = q_0 \exp[-\pi(j\Delta t/t_p - 1)^2] . \quad (12)$$

Obviously, the error from the truncation of the difference equations is $o(\Delta t + (\Delta x)^2)$. As an example of the gold target, we simulate the target temperature evolvment before laser ablating. The thermal and optical properties of the gold are presented in Tab.1.

Tab.1 Thermal and optical properties of the gold

| $k_e(\text{wm}^{-1}\text{k}^{-1})$ | $C_e(\text{Jm}^{-3}\text{k}^{-2})$ | $C_i(\text{Jm}^{-3}\text{k}^{-1})$ | $b(\text{m}^{-1})$ | $g(\text{wm}^{-3}\text{k}^{-1})$ | R |
|------------------------------------|------------------------------------|------------------------------------|--------------------------|----------------------------------|---|
| 3.18 ^[19] | 67.7 ^[19] | 2.30 ^[19] | $7.88 \times 10^{7[19]}$ | $2.1 \times 10^{16[19]}$ | 0.94(770nm) ^[20] 0.98(1053nm) ^[19] |

Supposing that the target is irradiated by a 170 fs, 1053 nm pulse at 0.145 J/cm² and the initial temperature is 300 K, we can obtain that the evolvement of the temperature of the ion and electron subsystem depends on the time and the depth, as shown in Fig.1.

In Fig.1(a), the electron temperature increases rapidly during the single pulse irradiation. And the electron tempera-

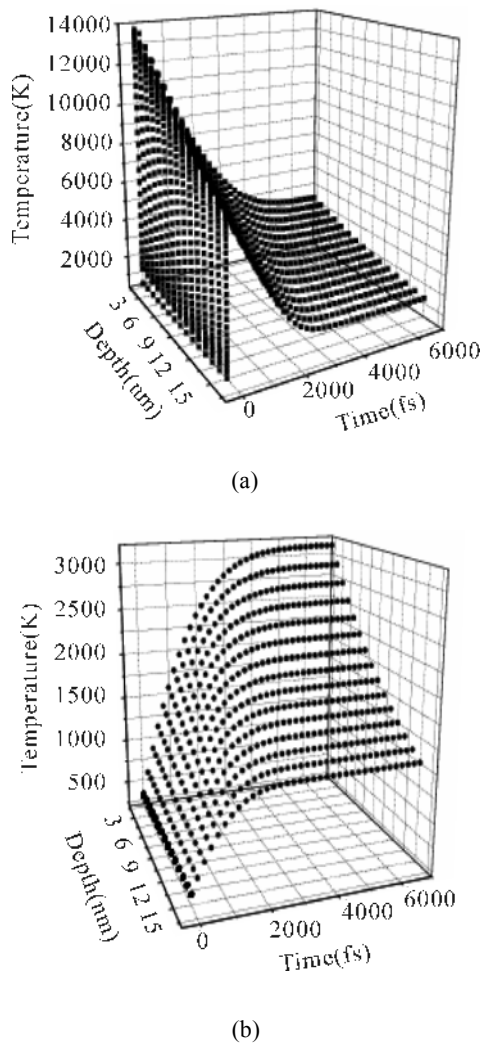


Fig.1 Temperature evolvement in the gold target. (a) the temperature evolvement of the electron subsystem, (b) the temperature evolvement of the ion subsystem.

ture decreases obviously while the laser stop irradiation. After t_{ie} , it is not changed and reduced slowly along with the depth.

As shown in Fig.1(b), the temperature of the ion subsystem rises gradually in t_{ie} . After that, the ion temperature changes slowly. But the ion temperature decreases more quickly than the electron temperature when the depth increases.

As a result, the temperature of the ion and electron subsystem combines one along with time, which accords with the experiment absolutely^[16].

Fig.2 presents the temporal evolvement of the temperature of the ion and electron subsystem in the gold surface during the laser irradiation. The electron absorbs laser energy and raises its temperature sharply during the laser irradiation. But the ion temperature is almost invariable. The tremendous difference of the temperature between the ion and the electron subsystem forms after 170 fs. Then the e-ph interaction plays an important role. The electron transfers energy to the ion. After the relaxation time of the electron-phonon interaction, the temperature of the ion and electron achieves the balance. In fact, the e-ph coupling time of gold is 6 ps from Fig.2.

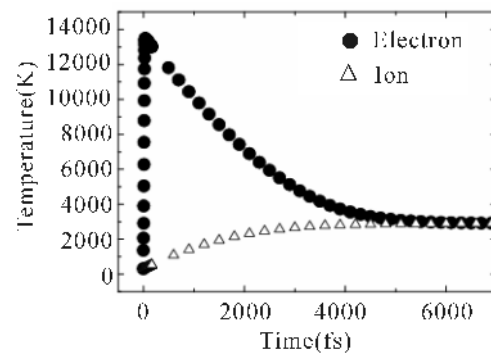


Fig.2 Electron and lattice temperature in the gold surface for the laser pulse width of 170 fs

Fig.3 presents the dependence of the temperature evolvement of the ion and the electron subsystem on the time in the gold surface for different pulse widths. The bigger the pulse width is, the lower the highest temperature of the electron subsystem is. But the maximum temperature of the electron subsystem almost does not change. Hence, the difference of the temperature between the ion and the electron subsystem decreases gradually. Finally, the temperature of the ion and

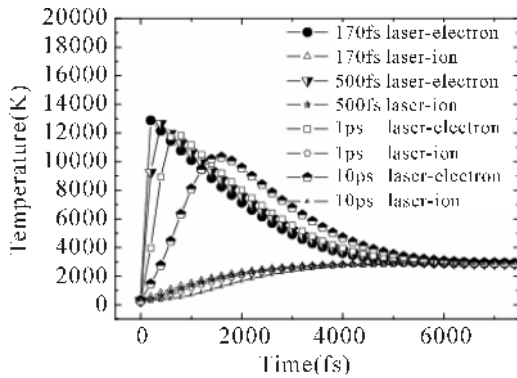


Fig.3 Temperature evolvement of the ion and electron subsystem for laser pulse widths of 170 fs, 500 fs, 1 ps and 10 ps

the electron subsystem is combined into one. Above all, the non-equilibrium ablation is changed into the thermal equilibrium ablation gradually when the laser pulse width is ranged from femtosecond to nanosecond.

Here, the critical temperature for the ablation is the corresponding temperature of the onset of a mass of evaporation.

For the short-pulse-laser ablated target, the evaporation has a close relation with the ionization. In the target surface, the mass is ionized quickly and the plasma is formed after the material is evaporated. The ionization temperature is higher than the evaporation one slightly. The ionization degree of 0.01% is considered as the onset of evaporation. Therefore, the temperature is considered as the critical temperature of laser ablation when the ionization degree is 0.01%. According to this assumption, we use the Saha equation to calculate the critical temperature of laser ablation. For the gold target, the critical temperature is 2873 K [17,18].

Generally, the laser ablation threshold is the laser energy corresponding to the onset of a mass of evaporation, i.e. the corresponding threshold temperature is 2873 K for gold target.

According to the above definition, we can ascertain the laser ablation threshold of gold. Fig.4 presents the dependence of the temperature evolvement of the ion subsystem on the time in the gold surface for the different threshold energies. Obviously, the curve corresponds to the laser energy one by one.

The temperature of each curve increases along with the time axis continually until achieving the maximum value at t_{ie} . The maximum value is the maximum temperature of the

ion subsystem. Factually, the ion temperature and electron temperature are combined into one at t_{ie} . The electron and the ion temperature arrive at the equilibrium temperature.

Hence, each curve has the maximum temperature which corresponds to the single laser ablation threshold only. If the maximum temperature of the ion equals to the threshold temperature of the laser ablation, the threshold energy for ablation will be ascertained. For the gold target, the laser ablation threshold corresponds to the maximum temperature 2873 K.

For a certain laser pulse width, the maximum temperature and the threshold energy can be ascertained. Fig.4 presents the dependence of the ion subsystem temperature evolvement on the time in the gold surface by a 1 ps laser irradiation. Hence, the laser ablation threshold is 0.43 J/cm² from Fig.4. Using this method, we can obtain a series of laser ablation thresholds with changing the pulse width.

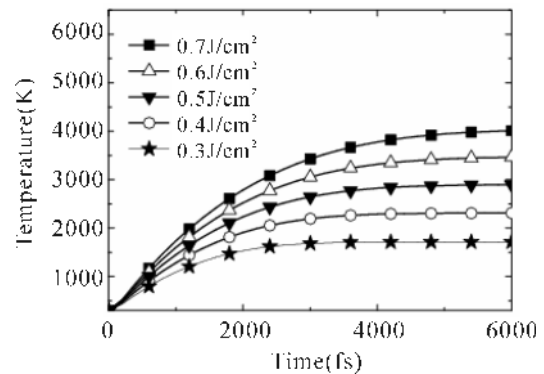


Fig.4 The temperature evolvement of the ion subsystem in the surface for different energies

Fig.5 presents the relation of the laser ablation threshold and the laser pulse width for a 1053 nm laser. Obviously, the computed results of the new unified model are in good agreement with the experimental data. It is better than the computed results of two-temperature models. The threshold energy of the unified model is close to the value of TTM for the laser pulse width $t_p \leq 1$ ps. The cause is that the non-equilibrium ablation is the most important part. It is obvious that unified model is the same as TTM for describing the ultra-short-laser ablated metal target. However, for $t_p > 1$ ps, the difference of the TTM theory is more than the one of unified model. The reason is that the thermal equilibrium ablation substitutes the non-equilibrium ablation gradually with the increase of the duration of pulse laser. It indicates that the

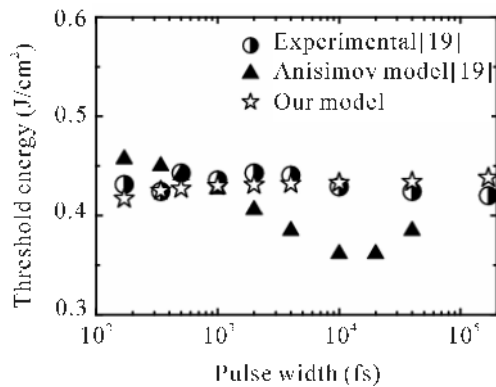


Fig.5 The relation of the laser ablation threshold and the laser pulse width for a 1053 nm laser

unified model can describe the thermal phenomenon of both non-equilibrium ablation and thermal equilibrium ablation.

Taking a further step, the laser wavelength is changed from 1053 nm to 770 nm. Fig.6 presents the relation of the laser ablation threshold and the laser pulse width for a 770 nm laser.

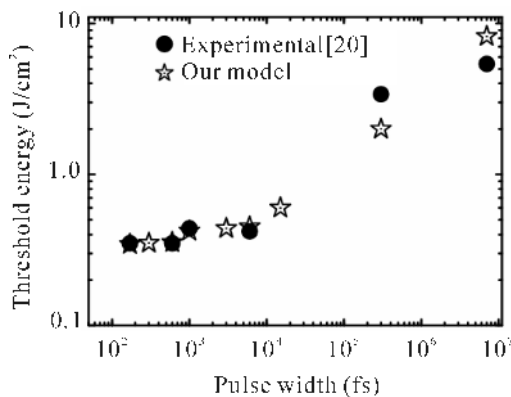


Fig.6 The relation of the laser ablation threshold and the laser pulse width for a 770 nm laser

It is shown that the theoretical results accord with the experimental data approximately. The unified model is available to describe the thermal conduction phenomenon of laser ablation for the laser with different wavelengths. However, the error increases obviously when the duration of the pulse laser is adjacent to the nanosecond timescale for the 770 nm

laser. The reason is that the reflectivity of the gold surface changes rapidly while the wavelength ranges from 500 nm to 800 nm. While the laser wavelength is larger than 800 nm, the reflectivity almost keeps constant at 0.98. Therefore, the result of the unified model is fully consistent with the experimental data at 1053 nm. We believe that the unified model can be modified further if the character of the reflectivity is considered.

In conclusion, this paper presents the unified model which describes the thermal conduction phenomenon in the process of laser ablation with the laser pulse width ranging from nanosecond to femtosecond timescale.

By using the Saha equation, we get the threshold temperature of the laser ablation. With the unified model, the dependence of the ion temperature evolution on the time in the gold surface is obtained.

For the laser wavelength larger than 800 nm, they are in consistence comparing the theoretical value with the experimental data of the laser ablation threshold. It shows that the unified model can describe the thermal conduction phenomenon in the process of laser ablation, where the laser pulse width ranges from nanosecond to femtosecond timescale. While the laser wavelength ranges from 500 nm to 800 nm, the error from the truncation between the theoretical value and the experimental data can not be neglected. It can be explained by the fluctuation of the reflectivity.

References

- [1] Zhang Duan-ming, and Li Li, et al., *Physic B*, **364** (2005), 285.
- [2] S. I. Anisimov, B. L. Kapeliovich, and T. L. Perelman, *Sov. Phys. JETP*, **39** (1975), 375.
- [3] S. Nolte, C. Momma, and H. Jacobs, *J. Opt. Soc. Am. B*, **14** (1997), 2716
- [4] C. Momma, and S. Nolte, *Applied Surface Science*, **109** (1997), 110
- [5] Zhang Duanming, Hou Sipu, and Guan Li, et al., *Acta Phys.*, **53** (2004),209.
- [6] Zhang DuanMing, Li Li, and Li ZhiHua, et al., *Acta Phys.* **54** (2005),1283.
- [7] Zhang Duanming, and Tan Xinyu, et al., *Physica B*, **V357**, **P348** (2005)
- [8] Li Guan, Zhang Duanming, and Hu Dezhi, et al., *Chin.Phys. Lett*, **23** (2006), 2277
- [9] Ki Hyungson, and Jyoti Mazumder, *Journal of laser applications*, **17** (1999), 110

- [10] T.W. Trelenberg, and L.N. Dinh, Applied Surface Science, 229(2004), 268
- [11] Yoichi Hirayama, and Minoru Obara, Journal of Applied Physics, **97** (2005), 064903
- [12] J.K.Chen, W.P.Latham., and J.E.Beraun, Journal of laser applications, **17** (2005), 63
- [13] Li Li, Zhang Duanming, and Hu Dezhi, et al., Physica B, **383** (2006), 194
- [14] A. Picciotto, and J. Kra, et al., Nuclear Instruments and Methods in Physics Research B, **247** (2006), 261
- [15] E. G. Gamaly, N. R. Madsen, and M. Duering, Physical Review B, **70** (2004),174405
- [16] R. Teghila, and L. D Alessioa, et al., Applied Surface Science, **210** (2003), 307
- [17] D.von der Linde, and K. Sokolowski Tinten, Applied Surface Science, **109** (2002),197
- [18] N. M. Bulgakova, Physical Review B, 69 (2004), 054102
- [19] Lan Jiang, and Hai-Lung Tsai, Journal of Heat Transfer, **127** (2005)1167
- [20] P. P. Pronko., S. K. Dutta, and D. Du, Journal of Applied Physics. **78** (1995), 15